The paper was published in the proceedings of the 10th International Conference on Scour and Erosion and was edited by John Rice, Xiaofeng Liu, Inthuorn Sasanakul, Martin McIlroy and Ming Xiao. The conference was originally scheduled to be held in Arlington, Virginia, USA, in November 2020, but due to the COVID-19 pandemic, it was held online from October 18th to October 21st 2021.

Effect of Fines Content on the Erosion Parameters of Gravelly Mixes

Ghada S. Ellithy[1], John. W. Murphy[2], Maureen K. Corcoran[3].

Affiliation: [1,2, 3] Engineer Research and Development Center, USACE, Vicksburg MS.

ABSTRACT

The mechanism and evolution of dam or levee breach caused by overtopping erosion is a complicated process. During the breach and overflow, erosion is difficult to measure due to accessibility and quick changing conditions. Erosion rate of soils during a levee or dam overtopping event is a major component in risk assessment when evaluating breach time, discharge rate and resulting downstream consequences. The results from flume erosion tests are presented and discussed in this paper. The tests are conducted in a 1-m (3-ft) wide tilting flume on six coarse-grained materials with a median grain size D_{50} of 2 mm and 20 mm and varying fines and clay content. The samples are prepared by compacting the soil mixes at or near the max dry density in a box embedded in the flume floor. The box measures 0.46 m wide x 1.22 m long x 0.18 m deep, and each soil mix is tested several times at varying flows and acting bed shear. A Shallow Water Lidar (SWL) system is utilized to record the evolution of soil erodibility and water depth along the scanned profiles of the test box under flowing conditions. The SWL is a noncontact system that transmits laser pulses from above the water and records the time-delay between top and bottom reflections. Results from the SWL scans are presented to show the effect of fines and clay content on the erosion rate as well as the effect of D_{50}. The change in erosion rate with acting bed shear is discussed in light of changing erosion depth.

INTRODUCTION

Erosion studies have been conducted in flumes where test boxes or small scale physical models are constructed and subjected to varying hydraulic loading to assess the erosion rate. Measurements of the eroded soil surface are typically taken before and after the test to quantify the erosion rate of the tested materials throughout the duration of the test. Real-time measurements of erosion during overflowing conditions would give a better understanding of the erosion evolution during the testing, however, such measurements have previously been difficult due to accessibility, quickly changing conditions, and lack of technology.

The physical phenomenon of erosion is complicated and is a function of the hydrodynamics of the hydraulic loading, the geomaterials that comprise the earthen structure as well as the geometry of the embankment. For flood risk assessment of both dams and levees, the earthen structures are assumed to breach when they are overtopped. However, for a more accurate assessment and to estimate a realistic time and width of breach, more understanding of the erosion rate and mechanism is needed especially for coarse-grained (or non-cohesive) sand and gravel materials.

For coarse-grained materials, the response of the particles to the hydraulic loading is mainly affected by the size, shape, and density of particles, while for the finer cohesive materials the response is affected by the cohesive bonding of the particles. The response of a mix of the two types of soils is governed by the relative fractions of the cohesive and non-cohesive particles. Cohesive or fine-grained materials have been studied more in terms of overtopping erosion, while uncertainty remains about the erosion parameters of coarse-grained materials.

This paper presents the results from soil erosion testing performed in a 0.91 m- (3 feet-) wide flume on four gravel soil mixes with varying fine contents compacted in a box built in the flume. A new Shallow Water Lidar (SWL) system was used to collect the soil erosion data under the water flowing conditions of each test. The data were processed and presented to illustrate the value of evaluating the erosion rate based on real time data throughout the test. Also, to present the effect of fines content and gravel particle size on the erosion rate.

MATERIAL PROPERTIES

Grain Size. The results presented in this paper are for three sand mixes: 1-1, 1-2, and 1-3 mod, and three gravel mixes: 1-7, 1-8 and 1-9 mod. The sand and gravel mixes maintain a D_{50} of 2 mm, and 20 mm, respectively as shown in Figure 1. Pea gravel, 25 –mm (1-inch) minus gravel, sands of different grain size distributions, silt, and kaolin clay materials were mixed in different proportions to produce these six mixes. The addition of the silt and clay to the clean sands and gravels in mixes 1-2 and 1-8 increased the fines to about 5 percent and the clay fraction ($<2\ \mu m$) to 1.5 percent. In mixes 1-3 mod and 1-9 mod, the increase in the fines and clay fraction was 15 and 5 percent, respectively. The plasticity index (PI) for the fraction passing sieve #40 was measured at 8% with a liquid limit LL of 26%. The uniformity coefficient: $C_u = D_{60}/D_{10}$, and the curvature coefficient; $C_c = D_{30}/D_{10} \times D_{60}$ were calculated for all the six mixes. Based on the above, the soil classification according to the unified soil classification system (USCS) for the six mixes

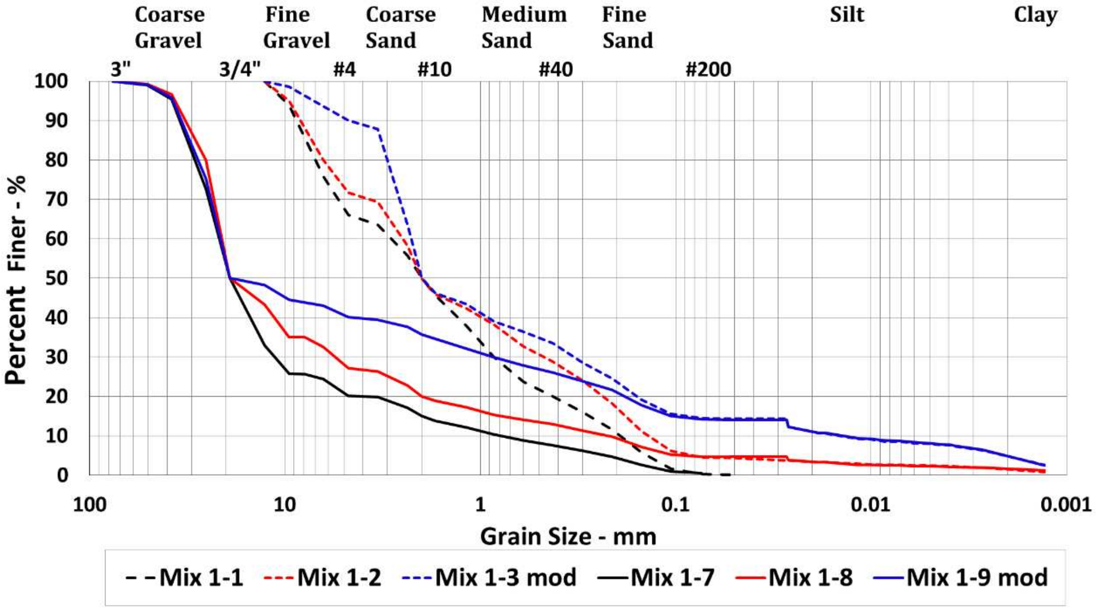

Figure 1. Grain size distribution for the six soil mixes

is: 1-1, well graded sand (SW),1-2, poorly graded sand (SP), 1-3 mod clayey sand (SC), 1-7, poorly graded gravel (GP), 1-8, poorly graded gravel (GP), and 1-9 mod, clayey gravel (GC).

Density and Compaction. To prepare the six mixes, compaction was performed according to the standard Proctor test (ASTM D698-12) for the sand mixes (1-1, 1-2, and 1-3 mod). For the gravel mixes (1-7, 1-8, and 1-9 mod) and since they contain larger size particles that are not permitted in the standard Proctor mold, a 30-cm (12-inch) diameter mold was used to compact the material at different moisture content using a 44.5-N (10-pound) hammer and number of lifts and blows to achieve the same energy as the standard Proctor method. The results of the compaction tests are shown in Figure . The dry density of the mixes increased with the fines content, however, the optimum water content remained within a narrow range between 3 and 6 percent. For the evaluation of soil mixes erodibility, density conditions were selected near optimum as shown in Table 1. Figure 2 shows these values in the circular symbols.

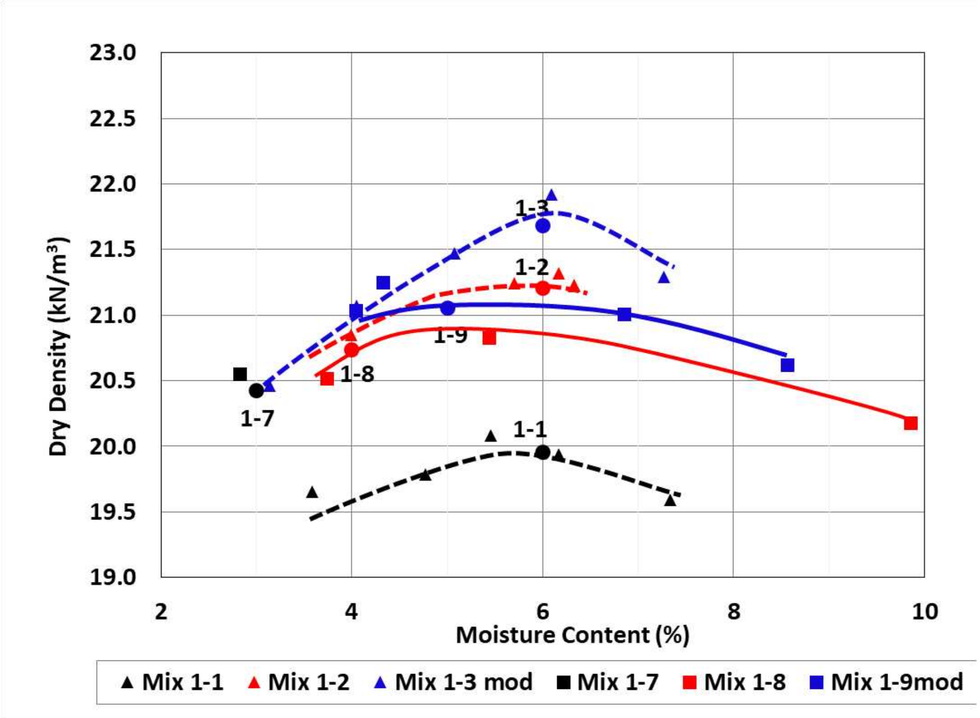

Figure 2. Compaction curves for the six soil mixes

FLUME TESTING SETUP

The flume that was used in this study measured about 18.3 m (60 feet) in length, 0.91 m (3 feet) in width and 0.46 m (1.5 feet) in height as shown in Figure 3. The flume bed could be tilted up to 8% (about 4.6 degrees) to achieve higher velocities at the same flow rate. A series of four variable speed pumps were used to adjust the flow rates in the flume. A flow ranging from 0.014 to 0.142 m^3/sec (0.5- 5.0 cfs) was used in performing the erosion tests for this study.

The flow width of the flume was narrowed from 0.91 m to 0.46 m (1.5 feet) starting 3.0 m (10 feet) upstream from the box and 1.83 m (6 feet) downstream. The test box is embedded in the flume bed and measures 1.22 m (4 feet) in length, 0.46 m (1.5 feet) in width and 0.18 m (7 inches) in depth. The soil sample was compacted in the box in two lifts, with calculated volume and weight to match the corresponding density and water content for each mix as mentioned above.

Before starting each test, the pumps were set to the selected flow level and the flume bed set to the slope. The flow continued in each test until sample erosion was observed to have reached an almost equilibrium condition where the erosion progress stopped or very slow erosion occurred. Prior to running the erosion tests, manual measurements of water depth with a sidewall mounted ruler and the velocity using a velocimeter were taken upstream, downstream and in the middle of the test box location at some flow rates and flume bed slopes. During the velocity measurements, an insert was placed into the box to create an even bed surface. A solution for the energy equation in the form of a first-order ordinary differential equation was calibrated against these measurements assuming a Manning's n value of 0.020. The average bed shear τ along the flume was then calculated using a discrete form of the momentum equation (Hughes 2017), more details on using this momentum equation are presented in Ellithy et al. 2018b.

Figure 3. Overview of the tilting flume.

SHALLOW WATER LIDAR (SWL)

A Shallow Water Lidar (SWL) system (ASTRALiTe Inc.) was used to take measurements of the soil and water depth during the erosion test. The SWL system works by transmitting laser pulses from above the water and recording the time-delay between top and bottom reflections. Figure 4 shows how the SWL unit was mounted to a railing system on which the unit was traveling parallel and perpendicular to the flow direction. The SWL was oriented vertically with the laser beam normal to the horizontal. It was assumed that the angle of reflection of the laser on the slopes that the flow was under will not affect the accuracy of the calculations. The railing system was about 0.75 m (2.5 feet) above the upper surface of the test box. An encoder was integrated in the railing system to measure horizontal position of the SWL parallel and perpendicular to the flow direction.

The traveling speed averaged about 0.75 m/ sec with an average acceleration of 1.0 m/sec^2. A laptop was set up to enable monitoring of the real-time data from the Lidar system. The plots generated from the real-time data were available throughout the test. The SWL scans were performed on eight profiles along the test box (parallel to the direction of the flow) the eight profiles are 0.025 m (1 inch) apart and cover the middle 0.18 m (7 inch) of the test box width. The SWL scanned each single profile along the box length of 1.22 m (4 feet) in 3.5 seconds, and completed each loop in about 27.5 seconds. The SWL collected readings with a pulse rate of 8000 Hz.

These raw surface data were post-processed by taking a mean value for a bin of 100 laser pulses to get an estimate of the distance to the soil surface. The data from the post-processing resulted in surface with ±1-cm vertical and horizontal precision. Prior to starting the erosion test, dry bed scans were taken by the SWL to be the datum of the scans taken during the test to calculate the erosion depth. Further calculations and data processing were performed using Matlab coding.

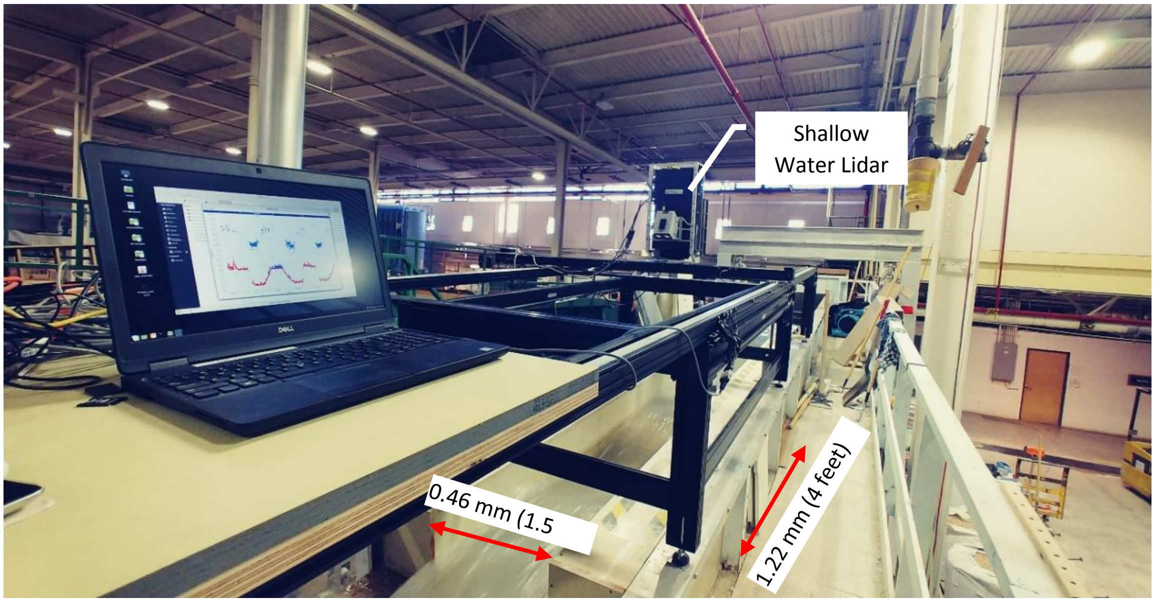

Figure 4. Shallow Water Lidar (SWL) system during performance.

RESULTS AND DISCUSSION

The SWL scanned the bed surface during each test. The flow rate and bed slope ranges tested for each mix are presented in Table 1, together with the calculated initial bed shear.

Soil Profiles. Figure 5 shows evolution of the bed surface with time for the center profile (profile 5) of the box for two selected tests. The soil surface for the first five passes (or loops) and the final pass are plotted against the distance from the initial scanning edge which is about 0.15 m from the downstream edge of the test box. The 1 m mark represents the top surface of the test box, where the bottom of the box is at 0.82 m depth. Spurious data points above 1 m were attributed to reflections off the water surface and suspended sediment.

Table 1. Summary of soil mix properties and test conditions.

Mix USCS	Gravel (%)	Sand (%)	Fines/ Clay (%)	D_{50} (mm)	As Compacted		Flow Rate (m^3/sec)	Slope (%)	Initial Average Bed Shear (Pa)
					Dry Density (kN/m^3)	Moisture Content (%)			
1-1 SW	34	66	0/ 0	2	19.9	6	0.014- 0.113	2	2.4- 22.3
1-2 SP	28	72	5/ 1.5	2	21.2	6	0.014- 0.062	2	2.4 – 19.8
1-3 mod SC	10	90	15/ 5	2	21.7	6	0.014- 0.062	6- 8	32.9- 50.6
1-7 GP	80	20	0/ 0	20	20.4	3	0.018- 0.117	2- 4	13.8-32.0
1-8 GP	73	27	5/ 1.5	20	20.7	4	0.018- 0.117	2-4	12.8- 22.4
1-9 mod GC	60	40	15/ 5	20	21.0	5	0.057- 0.139	6-8	32.9- 50.3

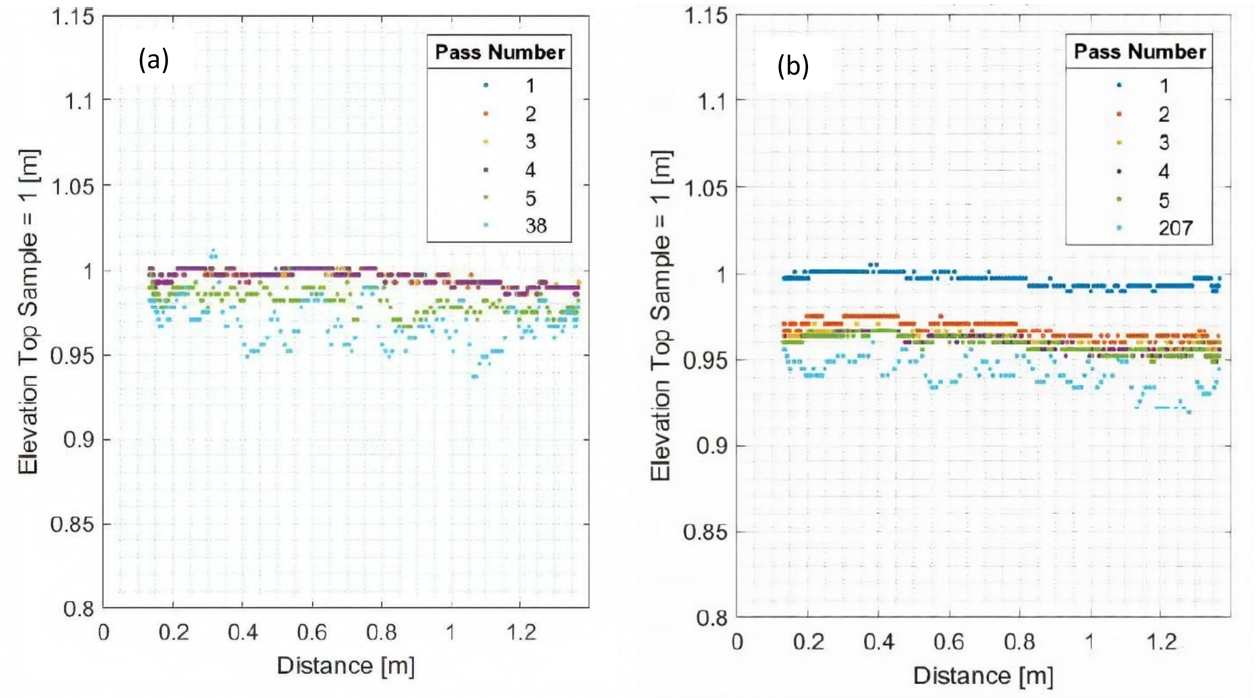

Figure 5: Soil surface along center profile for each loop versus distance from downstream end of scanning edge. (a) mix 1-7 (Q= 0.018m^3/sec, S=4%, shear=13.8 Pa), (b) mix 1-9 mod (Q=0.090 m^3/sec, S=6%, shear=40.0 Pa)

By a quick examination of the soil profiles plotted in Figure 5 for the two selected tests of mix 1-7 and 1-9, it could be observed that the number of passes required to achieve the same erosion depth was 207 for mix 1-9 mod which contained 5% clay content compared to 36 passes for mix 1-7 which contains no fines. This emphasize the role of fines in slowing the erosion process of soils given that mix 1-9 mod was tested at a higher initial bed shear of 40.0 Pa compared to mix 1-7 tested at 13.8 Pa.

Erosion Rate. The erosion rate shown in Figure 6 for the six soil mixes is calculated by dividing the difference between the initial soil elevation of the point of max erosion and the min soil elevation along profile 5 by the corresponding scan time. As it is shown in Figure 6 and summarized in Table 2, the erosion rate is reduced significantly with time for all the mixes as erosion depth increases and the scour hole forms. In the first 200 seconds (3.3 minutes), the reduction ranges from twice to an order of magnitude. After 800 seconds (13.3 min), the erosion has reach equilibrium and no erosion is recorded. This reduction in erosion rate could not be calculated if the erosion measurements are not taken at small time intervals from the beginning of the test which was facilitated by the use of the SWL system. If the time intervals were larger, a significantly lower erosion rate would have been calculated. This reduction could have been caused by the changes in the acting hydraulic loading and bed shear while the soil erosion is progressing.

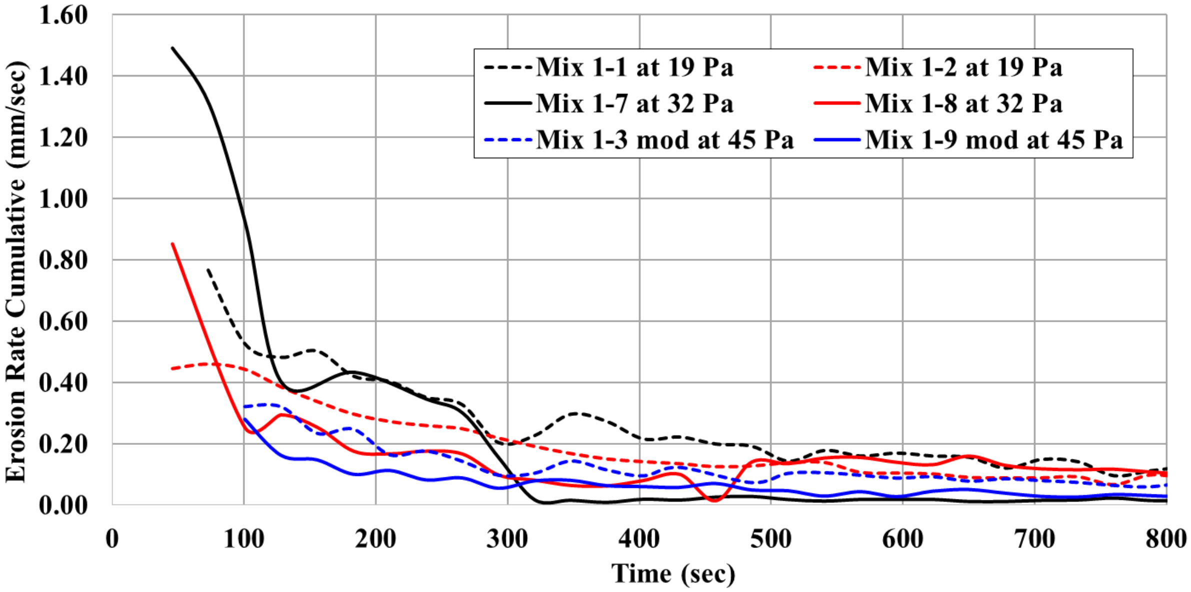

Figure 6: Erosion rate with time.

The erosion rate for mixes 1-1 and 1-2 is plotted at an initial bed shear of 19 Pa. It could be noticed that the increase of fines and clay content of 5 and 1.5 percent, respectively, in mix 1-2 compared to mix 1-1 which is a clean mix with no fines, resulted in a decrease in the initial erosion rate of about 40% from 0.74 mm/sec for mix 1-1 to 0.44 mm/sec for mix 1-2.

Table 2. Summary of erosion rate in mm/sec.

Time (s)	Mix 1-1	Mix 1-2	Mix 1-3 mod	Mix 1-7	Mix 1-8	Mix 1-9 mod
Initial	0.76	0.44	1.13	1.49	0.85	0.66
200	0.42	0.27	0.13	0.38	0.17	0.12
800	0.12	0.08	0.06	0.01	0.01	0.02

For mixes 1-7 and 1-8 the erosion rate is plotted at an initial bed shear of about 32 Pa. Mix 1-8 compared to mix 1-7 is similar to mix 1-2 to 1-1 with respect to the fines and clay content. Similarly, the fines and clay content presence resulted in a decrease in the initial erosion rate of about 43% from 1.49 mm/sec for mix 1-7 to 0.85 mm/sec for mix 1-8. The erosion rate for mixes 1-3 mod and 1-9 mod is plotted at an initial bed shear of about 45 Pa. Both mixes have a higher fines clay content compared to the other mixes of 15% and 5 percent, respectively. It could noticed that the erosion rate for both mixes is close, yet the erosion for rate of mix 1-3 is higher which is related to the smaller particle size of the grain size distribution of this mix compared to mix 1-9 and the smaller D_{50}.

Figure 7 shows the initial erosion rate of the six mixes along the range of the initial bed shear stress they were tested under. In general, it could be noticed that in all the cases, the erosion rate decreases as the fines and clay content increase, i.e., comparing mixes 1-1 to 1-2 to 1-3 mod, and mixes 1-7 to 1-8 to 1-9 mod. Also, it could be notices that the mixes of smaller D_{50} of 2 mm, tend to erode quicker or have a higher erosion rate compared to those of larger D_{50} of 20 mm with the same fines and clay content, i.e., comparing mix 1-1 to 1-7, mix 1-2 to 1-8, and mix 1-3 mod to 1-9 mod. This should be expected as the larger particles will be resisting the movement and the smaller particle size would be dislodged faster at the same acting bed shear. It could be noticed also that by increasing the fines and clay content, the difference in erosion rate between the mixes with D_{50} of 2 mm and mixes with D_{50} of 20 mm becomes smaller.

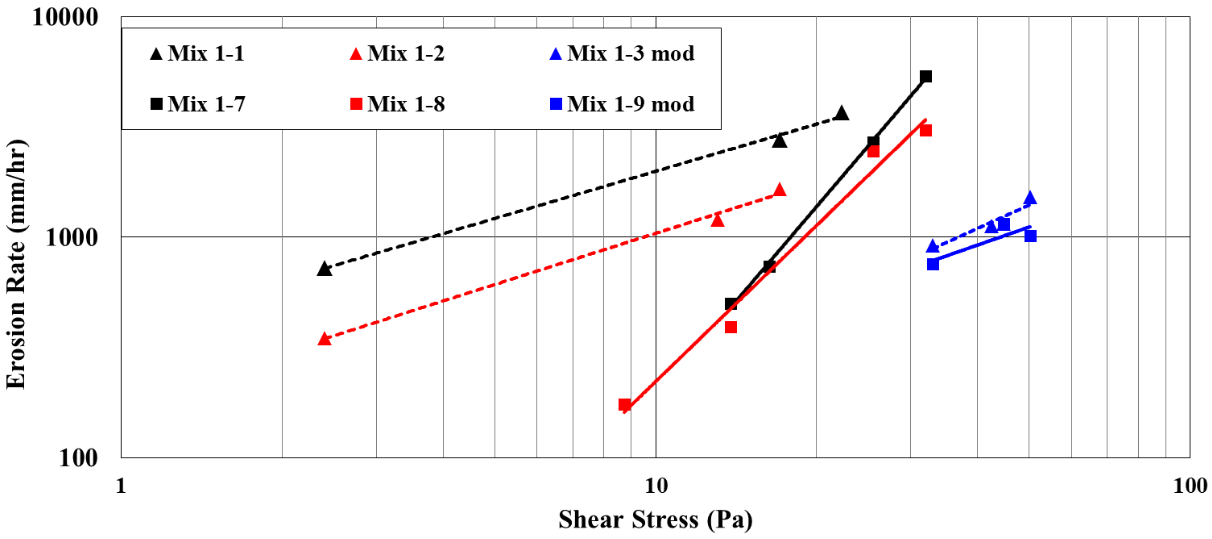

Figure 7: Initial erosion rate in mm/hr.

The erosion rate results of each mix were fitted by power equation in the form of ε=a τ^b where ε is the erosion rate in [L/T], τ is the acting initial bed shear stress in [F/L^2] and a and b are fitting constants. In this format, a and b will have dimensions and it is suggested that a normalized form of the equation is used (Ellithy, 2018a). This power form was found to be the most fitting for to the data points (R^2 = 0.93) compared to other known formulas like the excess shear equation (linear) or bilinear equation. These results are in line with conclusions from previous similar experiments like, Hanson and Simon 2001, van Rijn 1984, van Rijn 1993, Visser et al. 1986, and Yalin 1977.

SUMMARY AND CONCLUSIONS

This paper summarizes the results from flume erosion tests on six sandy and gravelly soil mixes with median size of 2 mm and 20 mm. The results presented in this paper indicate that the erosion rate significantly decreases with time as the scour hole forms and erosion reaches equilibrium. This reduction could not be calculated if the erosion measurements are not taken at small time intervals from the beginning of the test which was facilitated by the use of the shallow-water Lidar (SWL) system. The initial erosion rate and the level of reduction over time is affected by the fines content and D_{50} of the soil mix.

The results indicated that the mixes of smaller D_{50} of 2 mm, tend to erode quicker or have a higher erosion rate at the same acting shear stress compared to those of larger D_{50} of 20 mm with the same fines and clay content. However, by increasing the fines and clay content, the difference in erosion rate between the mixes with D_{50} of 2 mm and mixes with D_{50} of 20 mm becomes smaller. The results also showed that a nonlinear relationship in the form of power equation seems to give the best fit of the erosion rate of the tested sandy and gravelly soils throughout a wider range of acting shear stress and could accommodate the effect of fines content and D_{50}.

The paper demonstrates the advantage of using the SWL system in scanning real time erosion process compared to before-after results from conventional measurements in flume experiments. The SWL system offers a new technology that can provide an added research capability in the field of surface and overtopping erosion. Further investigation on the results from this soil erosion study will be conducted especially on quantifying the power equation constants and the effect of D_{50} and fines content on their values.

ACKNOWLEGMENT

The authors would like to acknowledge Tony Wahl and Christopher (Kit) Shupe of the US Bureau of Reclamation, Denver, CO for their continuous support and enormous assistance and efforts with the testing conducted for this study.

REFERENCES

ASTM. (2012). "Standard test method for Laboratory Characteristics of Soil Using Standard Effort (12,400 ft-lbf/ft^3 (600 kN-m/m^3)." American Society for Testing and Materials Standard Designation D 698-12, West Conshohocken, PA.

ASTM. (2007). "Standard test method for erodibility determination of soil in the field or in the laboratory by the Jet Index method." American Society for Testing and Materials Standard Designation D 5852-07, West Conshohocken, PA.

ASTRALiTe Atmospheric & Space Technology Research Associates, LLC (ASTRA). (2017). Erosion Flume Test – First Test Report USACE ERDC Test report (unpublished) www.astralite.net

Ellithy, G.S., Murphy, Corcoran, M.K. (2020). "Evaluation of Erosion Rate of Coarse-grained Materials Using a New Lidar Technology", GeoCongress 2020, Minneapolis, Feb24-28

Ellithy, G.S., Wibowo, J.L., Corcoran, M.K. (2018a). "Erosion Rate Equations for Coarse-Grained Materials Using a Small Flume Testing", of the 9th International Scour and Erosion (ICSE 2018), Taipei, Taiwan, November 5 – 8, 2018, 113.

Ellithy, G.S., Wibowo, J.L. Corcoran, M.K. (2018b). "Determination of Erosion Parameters of Coarse- Grained Materials Using a Small Flume", *Protections 2018 Conf Proceedings, UK*. 6-8June.

Hanson, G.J., and Simon, A. (2001). "Erodibility of cohesive streambeds in the loess area of the Midwestern, USA". Hydrological Processes, p 23-38.

Hughes, S.A. (2017). "Review of Proposed Physical Model to Evaluate Overtopping Erosion of Coarse-grained Materials". Report prepared for ERDC, water resources infrastructure technical program.

van Rijn, L.C. (1984). "Sediment pick-up functions." *Journal of Hydraulic Engineering* 110(10), 1494-1502.

van Rijn, L.C. (1993). "Principle of sediment transport in rivers, estuaries, coastal seas." Aqua Publications, Amsterdam, The Netherlands.

Visser, P.J., Ribberink, J.S., and Kalkwijk, J.P.Th. (1986). "Development of the breach and flow discharge in a dike-burst". Rep. 8-86, Hydraulic and Geotechnical Eng. Div., Dept. Civ. Eng., Delft Univ. Tehn., Delft, The Netherlands.

Yalin, M.S. (1977). "Mechanics of sediment transport". Pergamon Press, Oxford, England.